

Supplemental Material for: ‘Solar cell heterojunctions for candidate absorbers enargite and bournonite from electronic band and lattice matching’

Suzanne K. Wallace^{a,b}, Keith T. Butler^c, Yoyo Hinuma^{d,e}, and Aron Walsh^{*b,f}

^a *Department of Chemistry, Centre for Sustainable Chemical Technologies, University of Bath, Claverton Down, Bath, BA2 7AY, UK*

^b *Department of Materials, Imperial College London, Exhibition Road, London SW7 2AZ, UK. Email: a.walsh@imperial.ac.uk*

^c *ISIS Neutron and Muon Source, Rutherford Appleton Laboratories, Didcot, Oxfordshire, OX11 0QX*

^d *Center for Frontier Science, Chiba University, Chiba 263-8522, Japan*

^e *Center for Materials Research by Information Integration, Research and Services Division of Materials Data and Integrated System, National Institute for Materials Science, Tsukuba 305-0047, Japan*

^f *Department of Materials Science and Engineering, Yonsei University, Seoul 03722, Korea*

1 Slab models

Symmetric and non-polar surface terminations for enargite (Cu_3AsS_4) and bournonite (CuPbSbS_3) cut using methodology in Ref. [2]. The VESTA[4] software package was used to create Fig. 1 and 2.

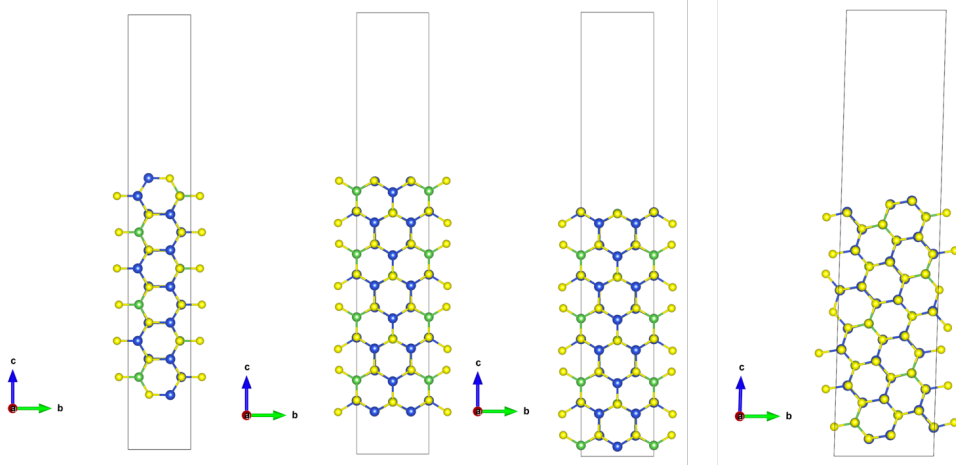


Figure 1: Enargite (Cu_3AsS_4) 100, 010a, 010b, 110 surface terminations.

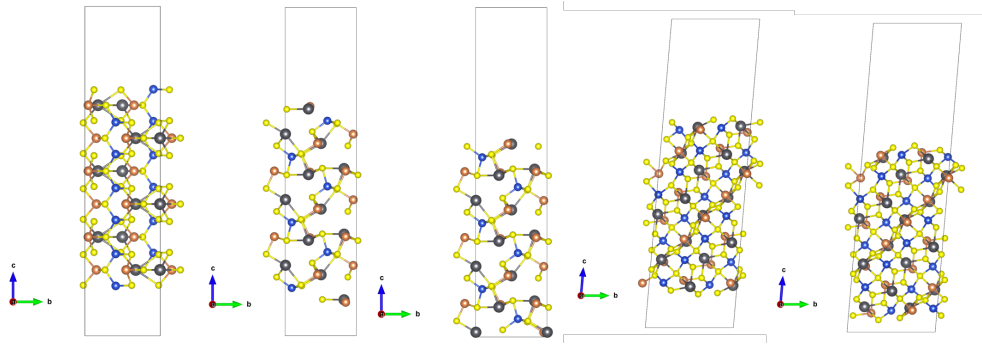


Figure 2: Bournonite (CuPbSbS_3) 100, 010a, 010b, 110a, 110b surface terminations.

2 Slab potentials

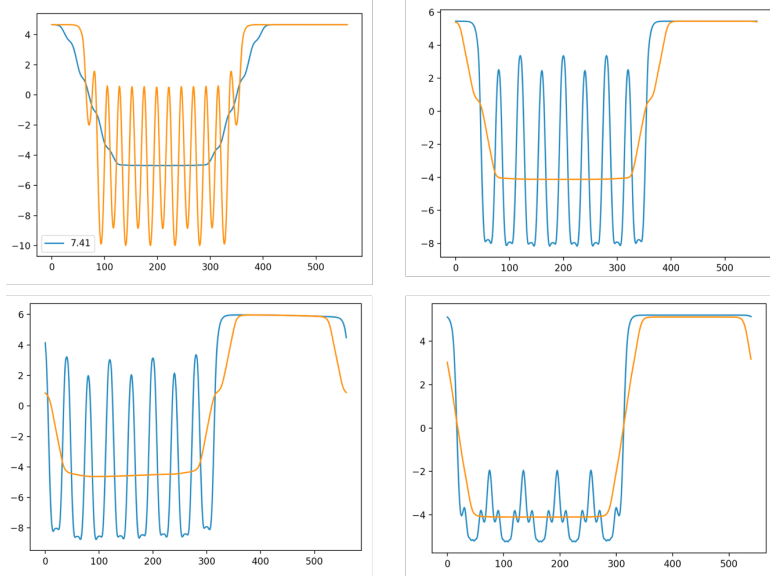


Figure 3: Enargite (Cu_3AsS_4) 100, 010a, 010b, 110 planar and macroscopic average electrostatic potentials using methodology from Ref. [3].

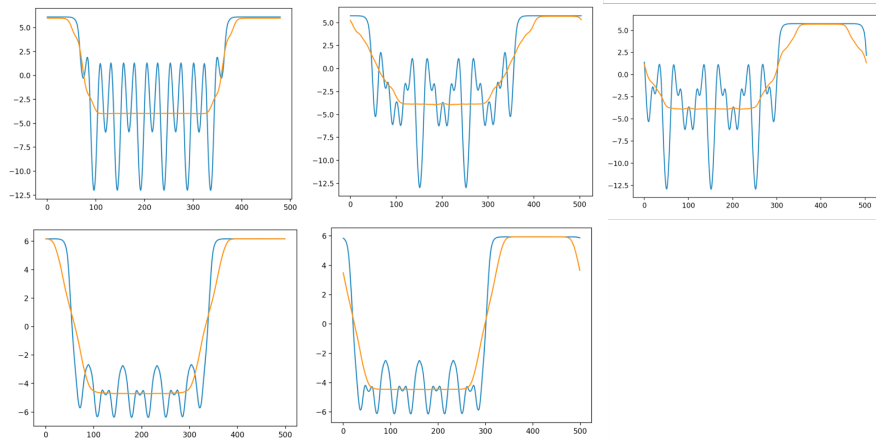


Figure 4: Bournonite (CuPbSbS_3) 100, 010a, 010b, 110a, 110b planar and macroscopic average electrostatic potentials using methodology from Ref. [3].

3 Structure files for junction partners used for lattice matching

Table 1: Materials project IDs for structure files used for lattice matching step.

Candidate	Materials project ID
Dy ₂ S ₃	mp-32826
La ₂ S ₃	mp-7475
Nd ₂ S ₃	mp-32586
Sm ₂ S ₃	mp-32645
Tb ₂ S ₃	mp-673644
WO ₃	mp-19033
ZnTe	mp-2176
Ce ₂ S ₃	mp-20973
Zn ₃ In ₂ S ₆	mp-637614
SiC	mp-11714
GaP	mp-2490
ZnSe	mp-1190
Ce ₂ O ₃	mp-542313
Bi ₂ O ₃	mp-23262
CoTiO ₃	mp-19424
NiTiO ₃	mp-556251
SnS ₂	mp-1170
Cu ₂ O	mp-361
Gd ₂ S ₃	mp-608146
AlP	mp-1550
MoO ₃	mp-18856
CuI	mp-570136
As ₂ S ₃	mp-641
CdS	mp-672
PbO	mp-19921
CoO	mp-24864

4 Band alignment with final junction partners candidates for all absorber slabs

Below are band alignment plots of the final junction partner candidates for each absorber layer slab. Ionisation potentials, electronic band gaps and electron affinities for the absorber materials are calculated in this work, but those of the candidate junction partners are from the dataset used in Ref. [1] and contained in the ELS git repository. The minimum strain termination for each junction partner candidate were shown in the main manuscript in Tables 2 and 3.

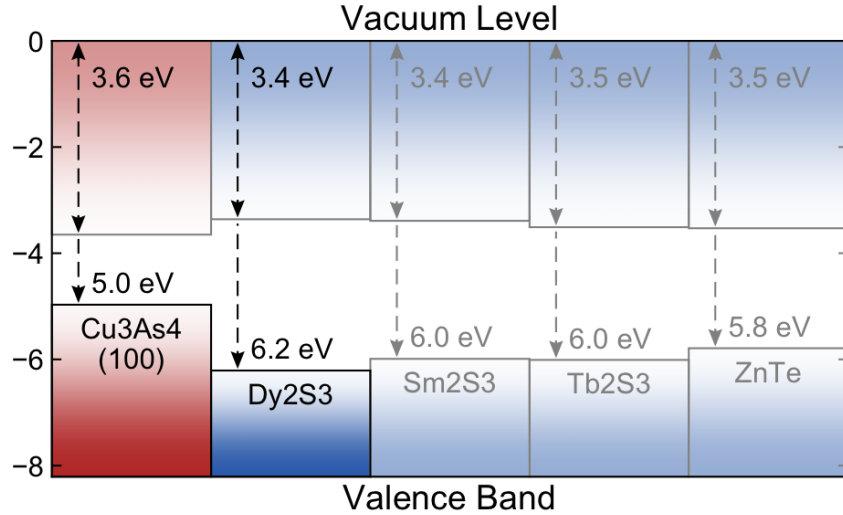


Figure 5: Spike conduction band offset (CBO) for enargite (Cu_3AsS_4) (100) termination.

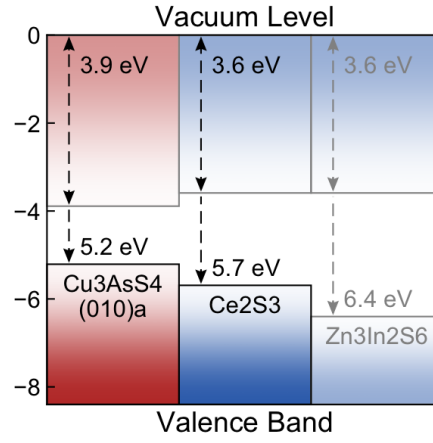


Figure 6: Spike conduction band offset (CBO) for enargite (Cu_3AsS_4) (010)a termination.

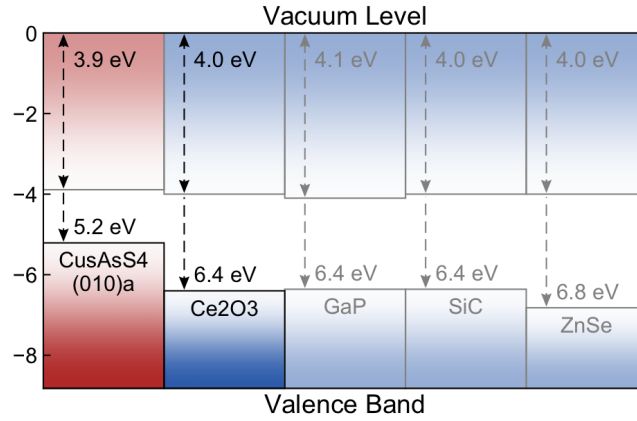


Figure 7: Cliff conduction band offset (CBO) for enargite (Cu_3AsS_4) (010)a termination.

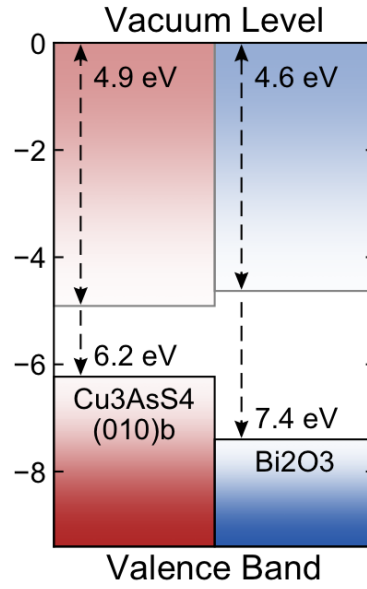


Figure 8: Spike conduction band offset (CBO) for enargite (Cu_3AsS_4) (010)b termination.

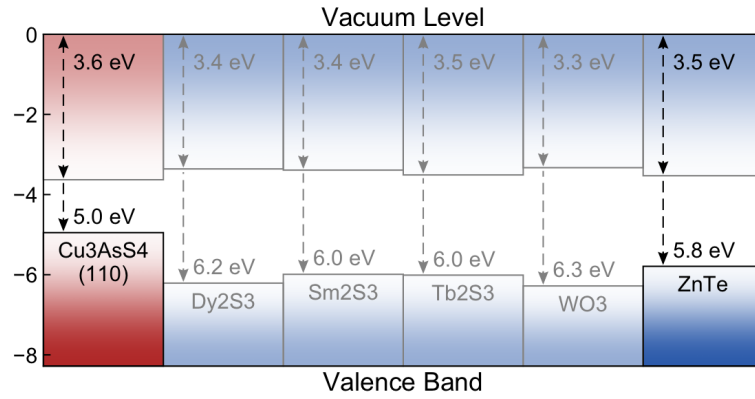


Figure 9: Spike conduction band offset (CBO) for enargite (Cu_3AsS_4) (110) termination.

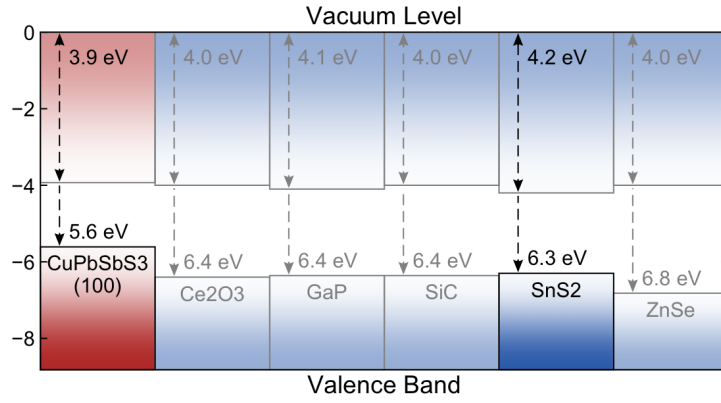


Figure 10: Cliff conduction band offset (CBO) for bournonite (CuPbSbS_3) (100) termination.

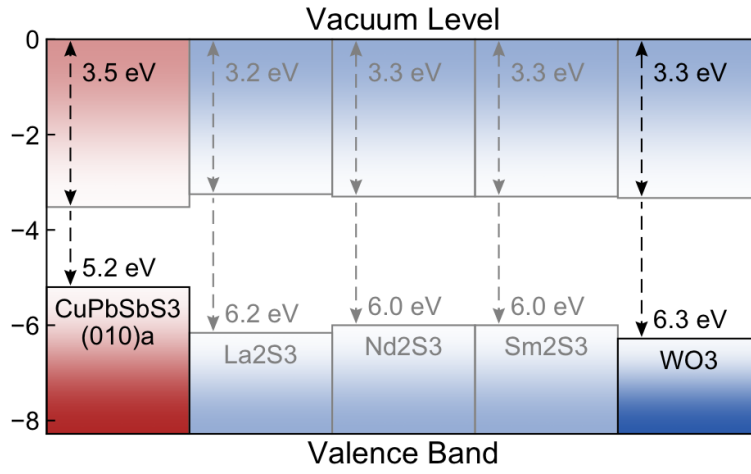


Figure 11: Spike conduction band offset (CBO) for bournonite (CuPbSbS_3) (010)a termination.

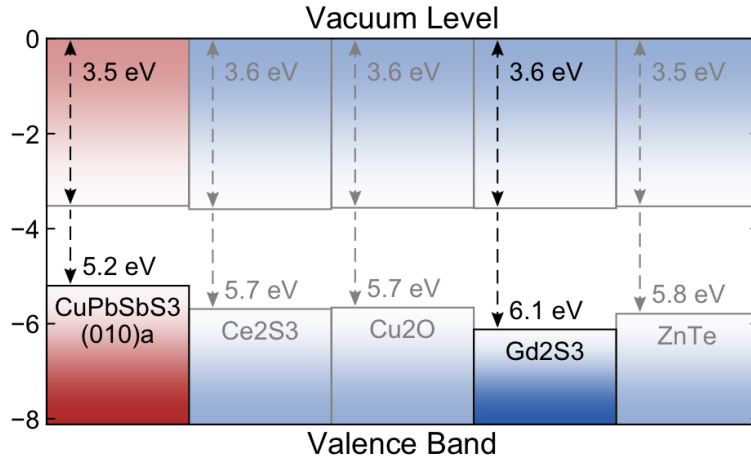


Figure 12: Cliff conduction band offset (CBO) for bournonite (CuPbSbS_3) (010)a termination.

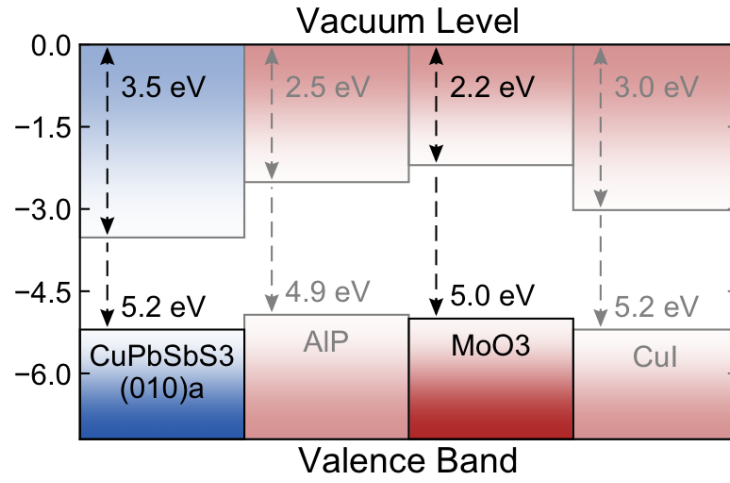


Figure 13: Cliff conduction band offset (VBO) for bournonite (CuPbSbS_3) (010)a termination.

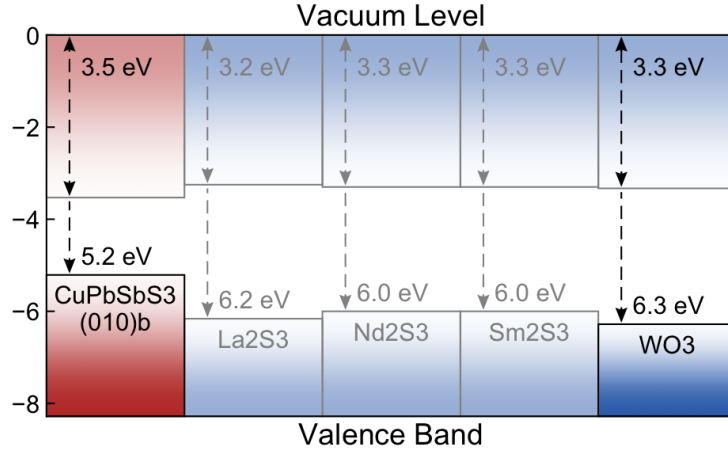


Figure 14: Spike conduction band offset (CBO) for bournonite (CuPbSbS_3) (010)b termination.

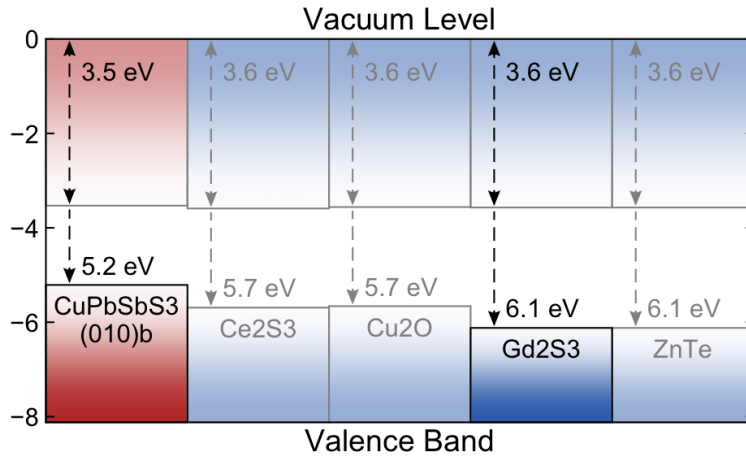


Figure 15: Cliff conduction band offset (CBO) for bournonite (CuPbSbS_3) (010)b termination.

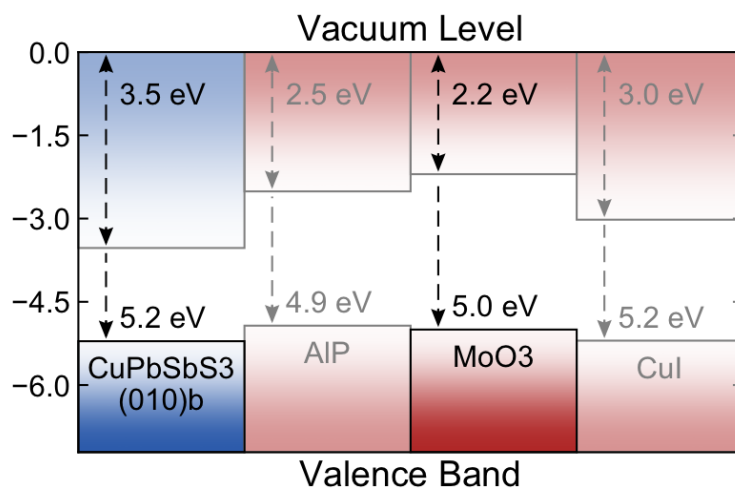


Figure 16: Cliff conduction band offset (VBO) for bournonite (CuPbSbS_3) (010)b termination.

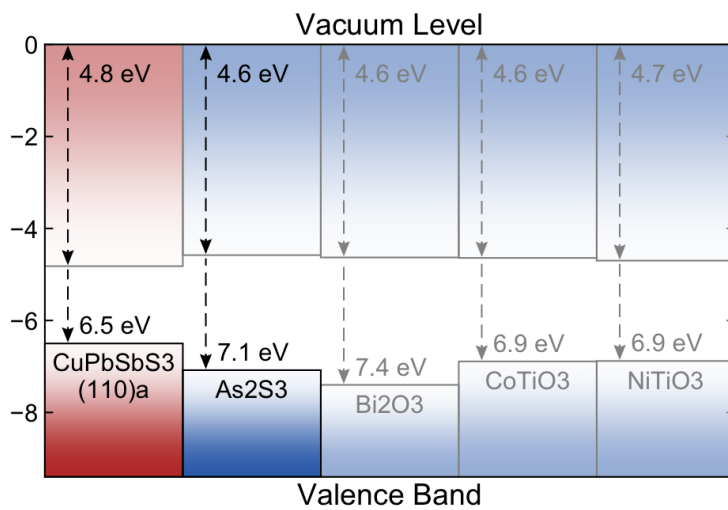


Figure 17: Spike conduction band offset (CBO) for bournonite (CuPbSbS_3) (110)a termination.

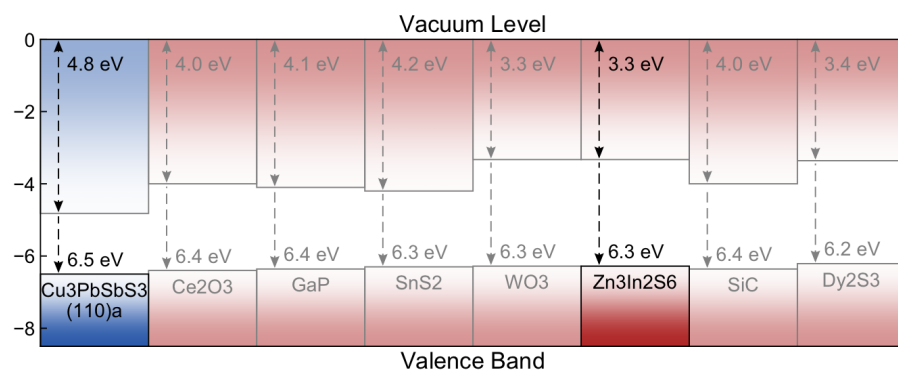


Figure 18: Cliff conduction band offset (VBO) for bournonite (CuPbSbS_3) (110)a termination.

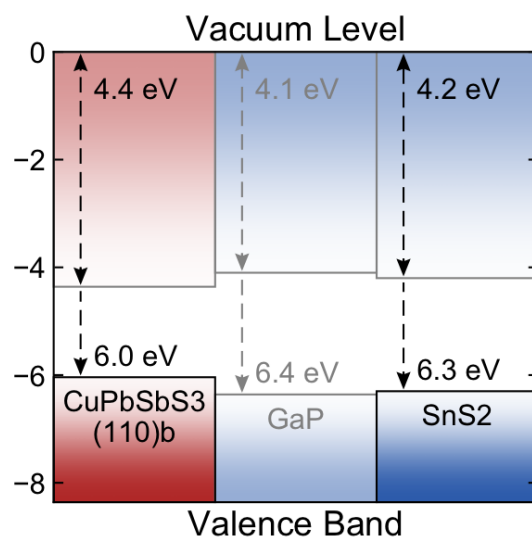


Figure 19: Spike conduction band offset (CBO) for bournonite (CuPbSbS_3) (110)b termination.

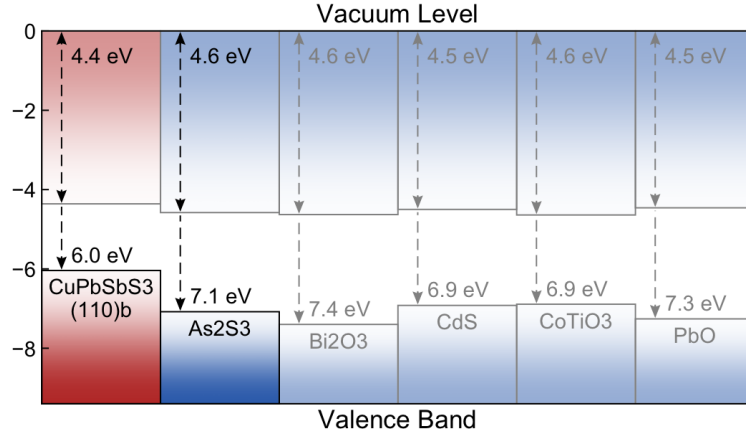


Figure 20: Cliff conduction band offset (CBO) for bournonite (CuPbSbS_3) (110)b termination.

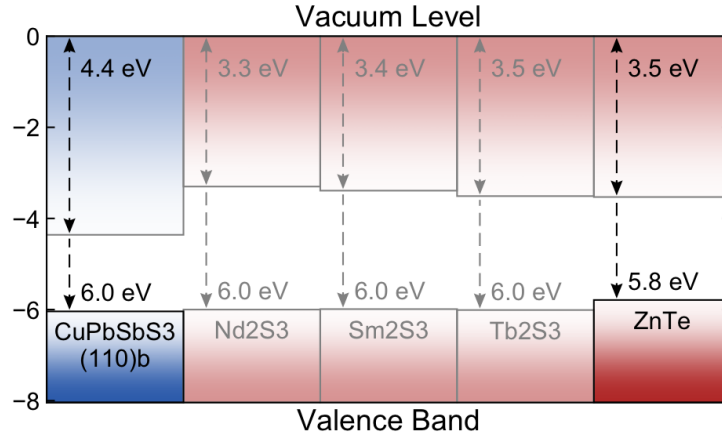


Figure 21: Cliff conduction band offset (VBO) for bournonite (CuPbSbS_3) (110)b termination.

References

- [1] K. T. Butler, Y. Kumagai, F. Oba, and A. Walsh. Screening procedure for structurally and electronically matched contact layers for high-performance solar cells: hybrid perovskites. *J. Mater. Chem. C*, 4(6):1149–1158, 2016.
- [2] Y. Hinuma, Y. Kumagai, F. Oba, and I. Tanaka. Categorization of surface polarity from a crystallographic approach. *Computational Materials Science*, 113:221 – 230, 2016.
- [3] Y. Kumagai, K. T. Butler, A. Walsh, and F. Oba. Theory of ionization potentials of nonmetallic solids. *Physical Review B*, 95(12), mar 2017.
- [4] K. Momma and F. Izumi. VESTA for three-dimensional visualization of crystal, volumetric and morphology data. *Journal of Applied Crystallography*, 44(6):1272–1276, oct 2011.